INBORN ERRORS *of* DEVELOPMENT

the molecular basis of clinical disorders of morphogenesis

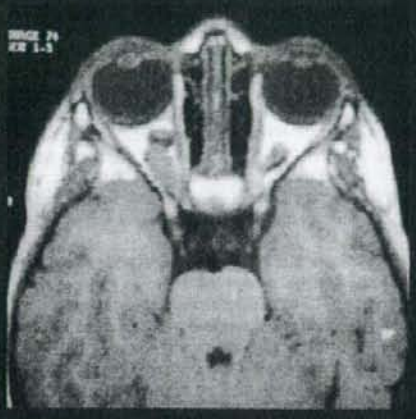

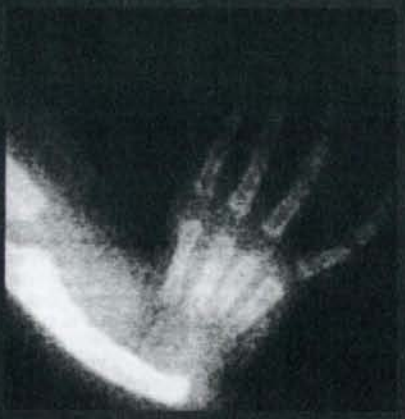

EDITED BY

Charles J. Epstein

Robert P. Erickson

Anthony Wynshaw-Boris

SECOND EDITION

113 | *NSD1* and Sotos Syndrome

REMCO VISSER AND NAOMICHI MATSUMOTO

Sotos syndrome (OMIM 117550) is a childhood overgrowth syndrome characterized by accelerated growth, typical craniofacial features, and a certain level of learning impairment. Sotos syndrome is caused by haploinsufficiency of the Nuclear receptor binding SET Domain protein 1 (*NSD1*) gene at 5q35.2-q35.3. Genetic analysis has established insight in the spectrum of genomic abnormalities of *NSD1*, in the underlying mechanisms of *NSD1* microdeletions and in the genotype–phenotype correlation in Sotos syndrome. However, the functional roles of NSD1 are yet largely unknown. A major role of NSD1 seems to lie in the transcriptional regulation of chromatin through the histone methyltransferase activity of its Su(var) 3–9, Enhancer of zeste, Trithorax (SET) domain. Furthermore, the nuclear receptor interacting domains (NIDs) are thought to be involved in transcriptional regulation by acting as both a coactivator and corepressor of nuclear receptors. Identification of interacting proteins and mapping of NSD1 into causative signaling pathways are the challenging future tasks in Sotos syndrome in order to clarify the link between genetic abnormalities and the Sotos phenotypic characteristics.

DEVELOPMENTAL PATHWAY

The *NSD1* gene is mapped to 5q35.2-q35.3 and consists of 23 exons. The open reading frame starts in the second exon, is 8088 bp long, and encodes 2696 amino acids. There are two known transcripts, a shorter variant 1 (7693 bp; GenBank accession number NM_172349) and a longer variant 2 (8458 bp; GenBank accession number NM_022455). The *NSD1* gene encodes a protein that consists of multiple functional domains; one Su(var) 3–9, Enhancer of zeste, Trithorax (SET) domain, a SET-associated cys-rich (SAC) domain, two proline–tryptophan–tryptophan–proline (PWWP) domains, five zinc-finger plant homeodomains (PHDs), a C5HCH domain and two nuclear receptor interaction domains (i.e., NID^{-L} and NID^{+L}) (see Fig. 113–1). The *NSD1* gene is expressed in the fetal and adult brain, skeletal muscle, kidney, spleen, thymus, lung, and in adult peripheral blood leukocytes (**Kurotaki et al., 2001**). *NSD1* belongs to a gene-family that includes *NSD2* and *NSD3* and shows approximately 75% and 70% sequence identity, respectively (**Kurotaki et al., 2001**). These genes possess similar functional domains, although NID^{-L} and NID^{+L} from *NSD1* are not present (**Stec et al., 1998; Angrand et al., 2001; Kurotaki et al., 2001**). Hemizygous deletions of *NSD2*, mapped to 4p16.3, are likely to be involved in the pathogenesis of the Wolf–Hirschhorn syndrome and translocations of *NSD2* have been described in multiple myeloma (**Stec et al., 1998**). *NSD3*, located at 8p12, has been found to be expressed in several tumor cell lines and in primary breast carcinomas (**Angrand et al., 2001**). Cryptic translocations resulting in fusions with the *nucleoporin 98 kDA* (*NUP98*) gene have been described in acute myeloid leukemia for both *NSD1* and *NSD3* (**Jaju et al., 2001; Rosati et al., 2002**).

The human *NSD1* shows 86% sequence similarity to the mouse *Nsd1* and 83% identity at the amino acid level (**Kurotaki et al., 2001**). Preceding the discovery of human NSD1, mouse Nsd1 was identified in a two-hybrid screen with retinoic acid receptor α as bait (**Huang et al., 1998**). It was found that Nsd1 interacted with nuclear hormone receptors through its nuclear interaction domains. These interactions occurred either in the absence of the ligand through NID^{-L} (retinoic acid receptor and thyroid receptor) or in presence of the ligand through NID^{+L} (retinoic receptor, thyroid receptor, retinoid X, and estrogen receptors). It was postulated that NSD1 could interact both as a corepressor and coactivator of nuclear receptors and would therefore be a bifunctional transcriptional regulator (**Huang et al., 1998**).

SET domain–containing proteins are known to function as histone methyltransferases at the chromatin level (**Kouzarides, 2002**). Cell experiments have shown that the SET domain of NSD1 exerts catalytic activity and methylates specifically histone H3 at lysine 36 (H3-K36) and histone H4 at lysine 20 (H4-K20) (**Rayasam et al., 2003**). Histone methylation at these specific positions has been associated with repression of chromatin transcription (**Rayasam et al., 2003**). Also PHD domains are predominantly found in proteins involved in chromatin regulation (**Aasland et al., 1995**). The PWWP domain is a protein–protein interaction domain, which exerts its function in cell differentiation (**Stec et al., 2000**).

Recently, an NSD1-interacting zinc-finger protein (Nizp1) was identified and a protein–protein interaction between its own C2HR motif and the NSD1 C5HCH domain was described (**Nielsen et al., 2004**). In an NSD1-dependent manner, Nizp1 showed transcriptional repressor activity (**Nielsen et al., 2004**). Abolishment of the Nizp1–NSD1 interaction significantly reduced this activity level of repression. Hence, either through its own domains or through interactions with Nizp1, NSD1 is likely to be involved in transcriptional regulation of chromatin.

In another study, the involvement of the growth hormone/insulin-like growth factor (GH/IGF) axis in the overgrowth in Sotos patients was investigated (**de Boer et al., 2004a**). In vitro experiments with skin fibroblasts from Sotos patients showed modestly increased levels of IGFBP-2 and IGFBP-6, as well as reduced levels of IGF-I, IGF-II, IGFBP-3, and IGFBP-4 (**de Boer et al., 2004a**). These changes would be more in accordance with a phenotype of short stature rather than tall stature and therefore the interpretation of these in vitro experiments, as well as the involvement of the GH/IGF axis in overgrowth in Sotos syndrome, requires further investigation.

CLINICAL DESCRIPTION OF *NSD1*–ASSOCIATED SYNDROMES

Sotos Syndrome

Sotos syndrome (OMIM 117550), formerly also known as cerebral gigantism, was first described in 1964 (**Sotos et al., 1964**). Since then, hundreds of cases have been reported. Until the discovery of *NSD1* as the causative gene, clinical criteria have been the standard for the diagnosis of Sotos syndrome (**Cole and Hughes, 1994**). Based on recent analyses of a large number of Sotos syndrome patients with a proven *NSD1* abnormality, the diagnostic criteria were redefined (**Douglas et al., 2003; Turkmen et al., 2003; de Boer et al., 2004b; Cecconi et al., 2005; Tatton-Brown et al., 2005b; Waggoner et al., 2005**). Cardinal features (i.e., ≥90% of the patients) for the diagnosis of Sotos syndrome are characteristic facial features, overgrowth (height and/or head circumference ≥98th percentile), and a certain degree of learning disability (**Tatton-Brown et al., 2005b**).

The typical Sotos craniofacial phenotype shows a triangular shaped ("inverted pear-like") face with a prominent chin, macrodolichocephaly, frontal bossing with a high hairline, (apparent) hypertelorism, and downslanting of the palpebral fissures (see Fig. 113–2). These features become less apparent in adolescence and adulthood, and therefore,

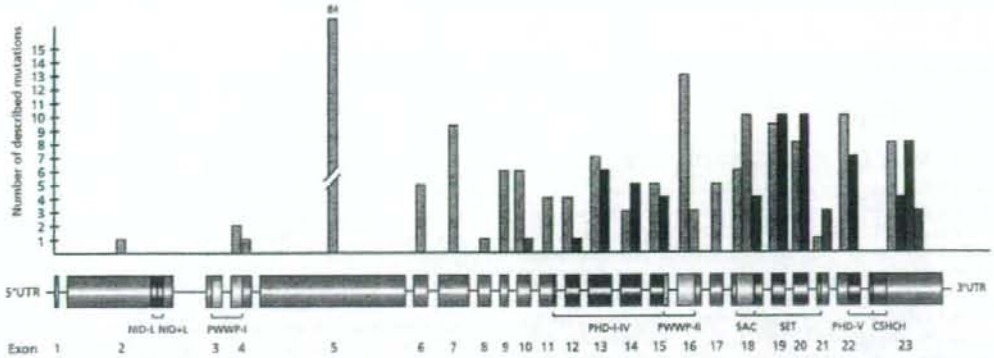

Figure 113–1. Schematic presentation of the *NSD1* structure with its functional domains and distribution of point mutations. The graph above represents the number of point mutations as described in the previous studies (**Kurotaki et al., 2003; de Boer et al., 2004b; Melchior et al., 2005; Tatton-Brown et al., 2005b; Tong et al., 2005; van Haelst et al., 2005**). The study from **Tatton-Brown et al., (2005b)** overlaps with those by **Cecconi et al. (2005)**, **Douglas et al. (2003)**, **Rio et al. (2003)**, **Turkmen et al. (2003)**, **Waggoner et al. (2005)**. The latter ones are, therefore, not included in this graph. Gray bars represent truncating mutations and colored bars indicate missense mutations in the respective functional domains (orange, dark-blue, light-blue, pink, and red) or outside the domains (green). From all studies, familial cases are counted as one single mutation and splice-site mutations are included in the truncating mutation group of the possibly affected exon.

photographs taken at infancy and in childhood are indispensable for diagnosis.

The growth pattern shows an accelerated growth, which starts prenatally or postnatally, and is especially increased in the early years of childhood. The final adult height, however, is found to be within the (high) normal range (**Tatton-Brown and Rahman, 2004**). Although overgrowth is a cardinal feature, children carrying a pathogenic *NSD1* mutation with normal heights have been described (**Tatton-Brown et al., 2005b**).

In a large study, 96% (112/117) of the Sotos syndrome patients showed a certain degree of learning disability (**Tatton-Brown and Rahman, 2004**). The range of mental impairment is usually broad, varying from mild to severe.

Furthermore, Sotos syndrome is associated with a large variety of additional features such as advanced bone age (76%), scoliosis (43%; 43/101), seizures (41%; 43/105), neonatal feeding problems (83%; 85/105), neonatal hyperbilirubinemia (71%; 61/85), neonatal hypotonia (84%; 76/91), cardiac (24%; 24/102) and genitourinary anomalies (19%; 17/91) (**Tatton-Brown and Rahman, 2004; Tatton-Brown et al., 2005b**). Tumors are not common in Sotos syndrome, although patients with different types of tumors have been reported (**Rahman, 2005**).

Weaver Syndrome

Clinically overlapping with Sotos syndrome is Weaver syndrome (OMIM 277590), which was initially described in 1974 (**Weaver et al., 1974**). Less than 100 patients have been reported in the literature so far. Weaver syndrome is characterized by prenatal or postnatal overgrowth, typical facial features (i.e., macrocephaly, flat occiput, hypertelorism, micrognathia, long and prominent philtrum, and large ears), developmental delay, a hoarse low-pitched cry, advanced bone age, and

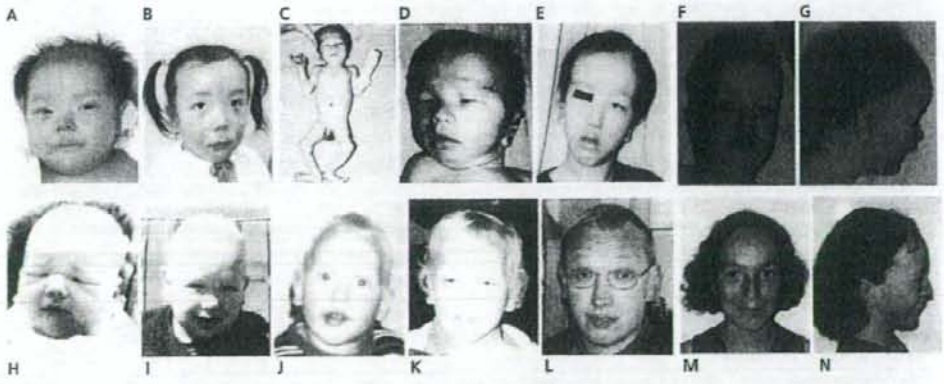

Figure 113–2. Facial features in Sotos syndrome patients with *NSD1* abnormalities. *(A)* and *(B)*: Japanese girl carrying a whole-gene microdeletion at the age of two months *(A)* and at three years *(B)*. *(C–E)*: A Japanese boy with a whole gene microdeletion at neonatal age [*(C)* and *(D)*] and at the age of six years *(E)*. *(F)* and *(G)*: Dutch girl with an *NSD1* nonsense mutation (c.1427T > A; p.L476X) at the age of 13 months. *(H)–(L)*: Dutch male with a whole-gene deletion at neonatal age *(H)*, at one year *(I)*, at two years *(J)*, at five years *(K)*, and at the age of 33 *(L)*. *(M)* and *(N)*: A ten year old girl from Moroccan ancestry carrying a missense mutation (c.6371G > A; p.C2124Y). [Photograph *(E)* was reproduced from Visser and Matsumoto, "Genetics of Sotos syndrome," *Curr opin Pediatr* 2003, 15(6): 598–606. With kind permission from the publisher Lippincott, Williams and Wilkins.]

finger- and nail abnormalities such as camptodactyly and deepset nails (**Cole et al., 1992; Opitz et al., 1998; Proud et al., 1998**). Due to the phenotypic overlap, distinction between Weaver and Sotos syndrome can be difficult (see further).

MOLECULAR GENETICS

Spectrum of *NSD1* Abnormalities in Sotos Syndrome

In 2002, a de novo balanced reciprocal translocation, 46,XX,t(5;8)(q35;q24.1), was described in a Japanese infant with Sotos syndrome (**Imaizumi et al., 2002**). Subsequently, the location of the breakpoint was mapped to 5q35.2-q35.3, disrupting the *NSD1* gene (**Kurotaki et al., 2002**). Within a Sotos syndrome group consisting of 42 Japanese individuals, four different de novo point mutations and 20 submicroscopic deletion mutations of *NSD1* were found (**Kurotaki et al., 2002**). Since then, several reports (see Table 113–1 and references) have shown that intragenic point mutations of *NSD1* are the main cause of Sotos syndrome in non-Japanese populations and that microdeletions of the whole *NSD1* gene account for nearly 10% of the cases. In contrast, these microdeletions are the major cause of Sotos syndrome in the Japanese populations, with point mutations only occurring in approximately 10%.

Although mutations resulting in protein truncation are found throughout the *NSD1* gene without specific hotspot locations, missense mutations are preferentially located in the functional domains of *NSD1* (see Fig. 113–1).

In addition, intragenic partial microdeletions of *NSD1*, comprising a single or multiple exons, were reported in 8 out of 124 individuals (6%) with a classic Sotos syndrome phenotype (**Douglas et al., 2005b**). Remaining causes of *NSD1* abnormalities could be intronic mutations affecting splicing or changes in the regulatory factors controlling the expression of *NSD1*, which cannot be detected with the present techniques. Despite the high detection rate (90%–93%) of *NSD1* abnormalities in certain studies (**Turkmen et al., 2003; Tatton-Brown et al., 2005b**), also genetic locus heterogeneity cannot be excluded totally. A recent study did not detect any sequence abnormalities or epigenetic changes of the *NSD1* promoter region in a group of 18 classical Sotos syndrome patients without any confirmed *NSD1* sequence abnormalities or gene deletions (**Visser et al., 2006**).

NSD1 Abnormalities in Other Overgrowth Syndromes

To date, only six Weaver syndrome patients have been described harboring an intragenic *NSD1* point mutation (**Douglas et al., 2003; Rio et al., 2003**) and the screening was negative in 16 additional patients (**Douglas et al., 2003; Rio et al., 2003; Turkmen et al., 2003; Cecconi et al., 2005; Tong et al., 2005**). Furthermore, the three patients from **Douglas et al. (2003)** initially described as Weaver syndrome were reclassified as typical Sotos (2) and Sotos-like (1) in a recent study (**Tatton-Brown et al., 2005b**). Therefore, it remains questionable whether *NSD1* abnormalities are responsible for classic Weaver syndrome, as is also noted by others (**Tatton-Brown et al., 2005b**).

Recently, two patients with Beckwith–Wiedemann syndrome (see Chapter 104) were reported to carry *NSD1* mutations (**Baujat et al., 2004**). Furthermore, a Japanese patient with Nevo syndrome and a submicroscopic deletion of *NSD1* was reported (**Kanemoto et al., 2006**). Additional patients are necessary to determine whether these cases are accidental (due to an overlap phenotype) or whether a small subgroup of these syndromes is caused by an *NSD1* abnormality.

NSD1 abnormalities were not detected in a large group of patients with a nonspecific overgrowth phenotype (**Douglas et al., 2003; Turkmen et al., 2003; Cecconi et al., 2005**). Because of the large number of patients screened to date, including populations with a broad range of phenotypes, it can be reasonably concluded that *NSD1* abnormalities are specific to Sotos syndrome.

Other Causes of Sotos Syndrome

In two patients with a Sotos syndrome phenotype, abnormalities were detected in the imprinted region on 11p15, which is associated with Beckwith–Wiedemann syndrome (**Baujat et al., 2004**). Although additional patients have yet to be reported, it is interesting to hypothesize that the histone methyltransferase activity of NSD1 could be a factor playing a role in establishing the parental imprint in this region (**Baujat et al., 2004**).

In 78 Sotos patients in whom *NSD1* abnormalities were excluded, the *NSD*-gene–family members *NSD2* and *NSD3* were screened but no mutations were found (**Douglas et al., 2005a**).

Mechanism of Submicroscopic Microdeletions of *NSD1*

The studies in the Japanese Sotos syndrome patients showed a high frequency of common approximately 2.2 Mb microdeletions, including *NSD1* and neighboring genes (**Kurotaki et al., 2002; Kurotaki et al., 2003**). The breakpoints occurred in flanking highly homologous genomic segments, so-called low-copy-repeats (LCRs) (**Kurotaki et al., 2003**). In six out of eight investigated cases, the meiotic rearrangement was of intrachromosomal origin and a preference was found for the paternally derived chromosome (18/20) (**Miyake et al., 2003**).

Table 113–1. Frequency of *NSD1* Mutations and Microdeletions in Sotos Syndrome[*]

Study	*NSD1* Abnormalities (%)	Intragenic Mutations (%)	Microdeletions (%)
Kurotaki et al., 2002	57 (24/42)	10 (4/42)	48 (20/42)
Douglas et al., 2003	64 (32/50)	58 (29/50)	6 (3/50)
Kamimura et al., 2003[†]	27 (8/30)	27 (8/30)	
Rio et al., 2003	67 (22/33)	48 (16/33)	18 (6/33)
Türkmen et al., 2003[‡]	90 (19/21)	90 (19/21)	0
Kurotaki et al., 2003[**]	59 (66/112)	14 (16/112)	45 (50/112)
Melchior et al., 2004	33 (11/33)	27 (9/33)	6 (2/33)
de Boer et al., 2004b[‡]	43 (23/53)	36 (19/53)	8 (4/53)
Cecconi et al., 2005	52 (17/33)	48 (16/33)	3 (1/33)
Tong et al., 2005	72 (26/36)	64 (23/36)	8 (3/36)
Waggoner et al., 2005[††]	13 (55/435)	21 (46/217)	2 (9/378)
Tatton-Brown et al., 2005b[‡‡]	93 (115/124)	77 (96/124)	10 (12/124)[***]

[*]No distinction is made between "classical" Sotos syndrome and "Sotos-like."
[†]Microdeletions were excluded before screening.
[‡]Familial cases are counted as one single mutation and only one patient per family is included.
[**]There is an overlap with the patient population from **Kurotaki et al., 2002**.
[††]Both *NSD1* mutation and deletion analyses were not performed in all patients.
[‡‡]From this study only the subjects from the United Kingdom are shown in order to exclude overlap with previous studies. There is a remaining overlap with the patient population from **Douglas et al., 2003**.
[***]Partial-gene deletions 6% (7/124) are not included.

The flanking LCRs were analyzed to have a high overall sequence similarity of approximately 98.5% and to be in an inverted orientation, except for an approximately 51 kb directly orientated region (see Fig. 113–3) (**Visser et al., 2005b**). The deletion breakpoints were mapped in approximately 79% (37/47) of a group of Japanese Sotos syndrome patients to a 3.0 kb recombination hotspot and the deletion size was refined to 1.9 Mb (**Visser et al., 2005b**). In another study, four additional deletion breakpoints were localized inside the directly orientated regions, but outside the Sotos recombination hotspot (**Visser et al., 2005a**). Nonallelic homologous recombination between the directly orientated regions (PLCR-B and DLCR-2B) was determined to be the underlying mechanism of the microdeletions (**Kurotaki et al., 2005a; Visser et al., 2005b**).

In a group of non-Japanese Sotos syndrome patients with a microdeletion size varying from 0.4 to 5.0 Mb, rearrangement occurred through an interchromosomal mechanism preferentially in the paternally derived chromosome (**Tatton-Brown et al., 2005a**). In contrast to the Japanese Sotos syndrome population, the detected microdeletion could have been mediated by the flanking Sotos LCRs in only 55% (18/33). For the remaining 45% (15/33), a microdeletion-causing mechanism differing from that in the Japanese population is likely (**Tatton-Brown et al., 2005a; Visser et al., 2005b**).

Since the Sotos syndrome LCRs are present in both the Japanese and non-Japanese population, it can be hypothesized that a specific genomic variation increases susceptibility for microdeletions in the Japanese population. A heterozygous inversion of the genomic interval between the Sotos LCRs was found in the parents [mothers 85% (11/13); fathers 100% (18/18)] of the Sotos patients carrying a microdeletion and also in a small Japanese control population [female 75% (3/4); male 67% (4/6)]. This inversion might interfere with meiotic pairing and consequently predispose to nonallelic homologous recombination (**Visser et al., 2005b**). However, further studies in Sotos syndrome and normal populations of different ancestry are necessary for elucidation of the prevalence and the role of this possible genomic inversion polymorphism.

Genotype–Phenotype Correlation in *NSD1* Abnormalities

In genotype–phenotype correlations in Sotos syndrome, an interesting point is whether Sotos characteristics are specifically attributable to *NSD1* abnormalities or whether neighboring dose-sensitive genes in the deleted segment contribute to additional features in Sotos syndrome. In an initial study consisting of five individuals harboring point mutations and 21 patients with a microdeletion, it was suggested that patients with a microdeletion showed a tendency to have smaller height and a more severe level of retardation than those with an intragenic mutation (**Nagai et al., 2003**). These results were confirmed in a study group comprised of 31 microdeletions and 208 intragenic mutations, which showed a significant difference for less-prominent overgrowth and more severe learning disability in the patients carrying microdeletions (**Tatton-Brown et al., 2005b**). The study by **Nagai et al. (2003)** also showed that some major anomalies in the central nervous, cardiovascular, and genitourinary system were only present in the microdeletion group. Although no significant difference in the prevalence of anomalies was found, a tendency toward more cardiac anomalies in the microdeletion group was observed by **Tatton-Brown et al. (2005b)**. In addition, there were no differences in associated features in relation to the different deletion sizes (**Tatton-Brown et al., 2005b**). A recent study showed that the plasma activity of coagulation factor 12 (FXII; also known as Hageman factor) in Sotos syndrome patients carrying a common deletion comprising *NSD1* and the *FXII* gene was correlated with a functional polymorphism of the nondeleted hemizygous *FXII* allele (**Kurotaki et al., 2005b**). Although the significance of the low level of FXII plasma

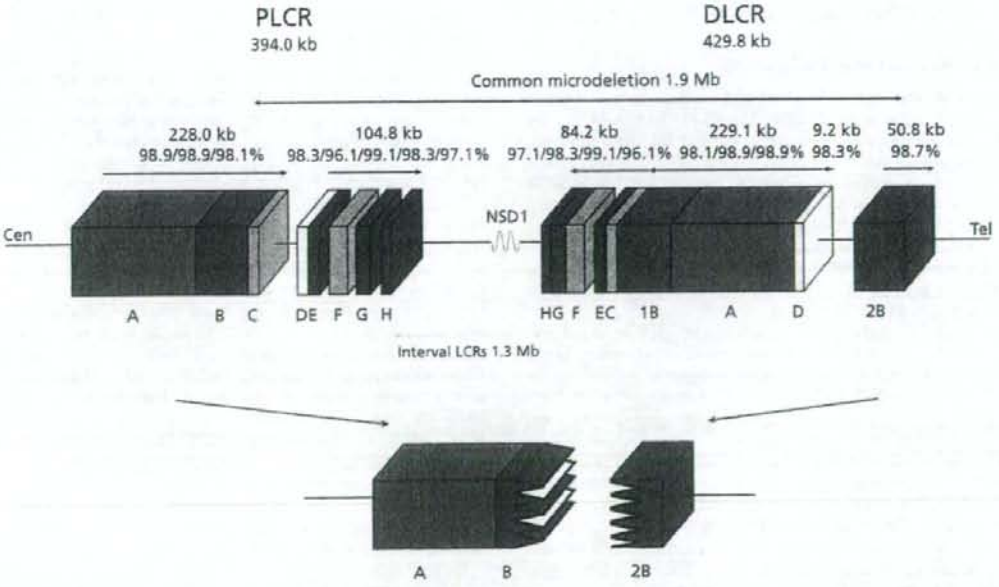

Figure 113–3. Schematic presentation of the two low copy repeats (LCRs) harboring the breakpoints of the common 1.9 Mb microdeletion in Sotos syndrome. In the lower part of the figure, the most common recombination (between PLCR-B and DLCR-2B) is shown. Blocks with the same color and same letter written below depict regions with sequence homology to each other. The size of (groups of) blocks and the sequence identity percentages are shown above the blocks. The direction of the horizontal arrows indicates the genomic orientation. The interval that might be involved in a predisposing inversion polymorphism (see text) is shown with an orange bidirectional arrow below the LCRs. (Fig. 113–3 is a modified version of Figure 1 from **Visser et al., 2005b** with kind permission from The University of Chicago Press, copyrights 2004 by The American Society of Human Genetics. All rights reserved.)

activity is yet unknown, its clinical consequences are considered to be small (**Kurotaki et al., 2005b**).

Since haploinsufficiency of the deleted genes in the microdeletion region has not been associated with specific additional features yet, it can be concluded that the Sotos phenotype is primarily caused by a reduced level of proper functioning NSD1.

DIAGNOSIS OF SOTOS SYNDROME

Nowadays, the diagnosis of Sotos syndrome is established by confirmation of *NSD1* abnormalities in patients with a phenotypical Sotos syndrome or with some Sotos syndrome characteristics. Analysis of *NSD1* includes at least the sequence analysis of exon 2–23 including exon–intron boundaries and either multiplex ligation probe amplification (MLPA) or fluorescent in situ hybridization (FISH) for possible deletions. MLPA is the preferred method for detection of intragenic and whole-gene deletions (**Douglas et al., 2005b**), while FISH analysis can be used for whole-gene deletions and investigation of the size of the broader deleted region (**Kurotaki et al., 2003**).

Because *NSD1* testing is now commonly available, physicians facing suspected patients should maintain a low threshold for *NSD1* testing. However, it is important to emphasize the importance of a good clinical diagnosis as the detection rate in a referral laboratory is significantly lower (13%) (**Waggoner et al., 2005**) compared to that in strictly diagnosed patient groups (90%–93%) (**Turkmen et al., 2003; Tatton-Brown et al., 2005b**).

Furthermore, screening of overgrowth patients without Sotos phenotypic features has not yet identified *NSD1* abnormalities (**Turkmen et al., 2003; Cecconi et al., 2005; Tatton-Brown et al., 2005b**). Therefore, standard screening of patients with a nonspecific overgrowth phenotype cannot be substantiated with the present literature. For patients with an overlapping phenotype of Beckwith–Wiedemann and Sotos syndromes, it is advisable to investigate both *NSD1* as well as 11p15 abnormalities (**Baujat et al., 2004**).

Although *NSD1* is not likely to be the causative gene of the classic Weaver syndrome, testing of *NSD1* is advised because the phenotypic differentiation from Sotos syndrome can be difficult. A negative result could also be used as an extra argument in favor of a classic Weaver syndrome diagnosis (**Tatton-Brown et al., 2005b**).

COUNSELING AND MANAGEMENT

Sotos syndrome is an autosomal dominant disorder with full penetrance (**Tatton-Brown et al., 2005b**). Therefore, the risk of vertical transmission is 50% when one of the parents is affected. However, most *NSD1* mutations occur de novo. The number of familial cases is lower than expected, suggesting a possible reduced fertility in Sotos patients (**Tatton-Brown et al., 2005b**). Missense mutations located outside the SET domain might be more common in familial mutations, although affected families with truncating mutations have also been reported (**Hoglund et al., 2003; Tatton-Brown et al., 2005b; Tong et al., 2005; Waggoner et al., 2005**). To date, no familial case has been described harboring an *NSD1* deletion.

At present, there is no specific treatment for the *NSD1* gene and protein defect in Sotos syndrome. Therefore, treatment is focused on the management of its manifestations. A large number of associated anomalies have been reported in Sotos syndrome patients (see earlier text), which require specific attention during anamnesis, physical examination, and additional investigations. Especially, at least possible cardiac (amongst others, atrial and ventricle septum defects) and urinary tract anomalies (e.g., vesicoureteral reflux and renal abnormalities) as well as musculoskeletal (for instance, scoliosis and pes planus) problems should be excluded. The incidence of tumors in Sotos syndrome is low (~2%), with a very low risk of malignant transformation (**Rahman, 2005**). Hence, no specific screening targeting tumors in Sotos syndrome other than normal examination seems necessary.

Learning impairment is one of the major criteria of Sotos syndrome and although not validated with *NSD1* analysis, behavior problems in general seem more frequent (**Sarimski, 2003**). Due to the large interindividual variation, it is important for the parents and caretakers to provide a proper (educational) environment for their child with an individualized approach.

MOUSE MODELS

In mice, *Nsd1* expression was seen at various developmental stages, with a ubiquitous expression pattern in both embryonic and extraembryonic tissue till embryonic day 14.5 (**Rayasam et al., 2003**). Subsequently, differential expression was observed in the telencephalic region of the brain, spinal cord, intestinal tooth buds, thymus, salivary glands, in the region of ossification of the developing bones, and in the periosteum (**Rayasam et al., 2003**). Heterozygous targeted $Nsd1^{+/-}$ mice did not to exhibit an apparent Sotos syndrome phenotype, although longer observation periods might be necessary for detection of subtle features (**Rayasam et al., 2003**). The lack of expression of *Nsd1* in mouse chondrocytes observed by **Rayasam et al.** might be an explanation for the lack of overgrowth in mice. Homozygous $Nsd1^{-/-}$ knockout mice died in utero before embryonic day 10.5. In these mutants, an abnormal gastrulation process was noted and Nsd1 is, therefore, thought to be crucial for early postimplantation development (**Rayasam et al., 2003**).

DEVELOPMENTAL PATHOGENESIS

Although the developmental pathogenesis in Sotos syndrome is not yet known, some lines of evidence suggest that NSD1 is associated with transcriptional regulation: first, the capacity to specifically methylate H3-K36 and H4-K20 and second, the interaction with Nizp1, which was shown to be a transcriptional repressor. Therefore, it is intriguing to hypothesize that haploinsufficiency of *NSD1* would result in the loss of transcriptional silencing of yet unknown growth promoting genes and consequently result in accelerated growth. It is presumed that NSD1 is influencing early stages of development since expression is found both in human fetal tissues as well as in mouse embryonic tissues, with Nsd1 being essential for early postimplantation development in mice (**Kurotaki et al., 2001; Rayasam et al., 2003**). In regard to these early expression patterns, overgrowth features and the facial gestalt can already be observed at birth, although the accelerated growth pattern and facial features are usually more pronounced in the early childhood. Considering the developmental delay in Sotos syndrome patients and a high prevalence (without confirmed *NSD1* analyses) of intracranial manifestations, such as enlarged ventricles, prominent trigone, and midline abnormalities (**Schaefer et al., 1997**), the normal neural development is likely to be affected.

How does an abrogated NSD1 function during the different stages of development result in the Sotos syndrome phenotype? One approach could be to construct a detailed phenotype–genotype correlation. However, such analysis would need a significant number of patients in combination with extensive clinical evaluation in order to also detect subtle differences. In general, no difference in phenotype–genotype correlation has been found so far between missense mutations and nonsense mutations in Sotos syndrome (**Tatton-Brown et al., 2005b**). Furthermore, different features were also found in patients with identical mutations (**Tatton-Brown et al., 2005b**). Mutations in familial cases are positioned outside the SET domain, implying a possible relationship of this domain with fertility (**Tatton-Brown et al., 2005b**). Although (because of this?) there are only about 25 familial cases to substantiate this observation (**Hoglund et al., 2003; Turkmen et al., 2003; de Boer et al., 2004b; Tatton-Brown et al., 2005b; Tong et al., 2005; van Haelst et al., 2005; Waggoner et al., 2005; Tei et al., 2006**). In submicroscopic microdeletions including *NSD1* and other genes, the net effect of phenotypic features seems to be attributable to the *NSD1* defect. In summary, the current data regarding the phenotype–genotype correlation are not sufficient to answer the questions related to the Sotos pathogenic pathway.

Establishing the functional network and protein interactions of NSD1 are more likely to create link between genetic abnormalities and the exhibited phenotype, and will yield insight in the underlying pathogenic mechanisms. So far, only Nizp1 has been identified as an interacting protein with NSD1. In addition, NSD1 is thought to act as a cofactor to nuclear hormone receptors in either a ligand dependent or

independent manner. The actual roles of these interactions in relation to the Sotos phenotype continue to be elusive. Identification of more upstream regulators and downstream effectors is necessary in order to be able to map NSD1 into a network of signaling pathways resulting in Sotos syndrome.

CONCLUSION

With the discovery of aberrations of the *NSD1* gene being responsible for Sotos syndrome, research focused on Sotos syndrome has made significant progress in increasing our understanding about the genetic background, the underlying mechanisms of the different *NSD1* abnormalities, and the genotype–phenotype relation. Only limited progress has been made in increasing insight into the possible functions of NSD1. A challenging task for future research projects will be the detailed analyses of these functional roles, identification of NSD1 targets, and unraveling of the signaling pathways in which NSD1 exerts its function(s).

ACKNOWLEDGMENTS

We are very grateful to the patients and parents for their permission to publish the photographs and to their physicians (Dr. S.G. Kant at the Department of Clinical Genetics, Leiden University Medical Center, Leiden, The Netherlands; Dr. N. Okamoto at the Department of Planning and Research, Osaka Medical Center and Research Institute for Maternal and Child Health, Izumi, Japan; and Dr. Y. Makita at the Department of Pediatrics, Asahikawa Medical College, Asahikawa, Japan) for their kind cooperation. R. Visser is supported by grant number 920-03-325 from The Netherlands Organization for Health Research and Development. His Sotos research is financially supported by Stinafo (Stichting Nationaal Fonds "Het Gehandicapte Kind").

References

Aasland R, et al. (1995). The PHD finger: implications for chromatin-mediated transcriptional regulation. *Trends Biochem Sci* 20(2): 56–59.

Angrand PO, et al. (2001). NSD3, a new SET domain-containing gene, maps to 8p12 and is amplified in human breast cancer cell lines. *Genomics* 74(1): 79–88.

Baujat G, et al. (2004). Paradoxical NSD1 mutations in Beckwith-Wiedemann syndrome and 11p15 anomalies in Sotos syndrome. *Am J Hum Genet* 74(4): 715–720.

Cecconi M, et al. (2005). Mutation analysis of the NSD1 gene in a group of 59 patients with congenital overgrowth. *Am J Med Genet A* 134(3): 247–253.

Cole TR, et al. (1992). Weaver syndrome. *J Med Genet* 29(5): 332–337.

Cole TR, Hughes HE (1994). Sotos syndrome: a study of the diagnostic criteria and natural history. *J Med Genet* 31(1): 20–32.

de Boer L, et al. (2004a). Mutations in the NSD1 gene in patients with Sotos syndrome associate with endocrine and paracrine alterations in the IGF system. *Eur J Endocrinol* 151(3): 333–341.

de Boer L, et al. (2004b). Genotype-phenotype correlation in patients suspected of having Sotos syndrome. *Horm Res* 62(4): 197–207.

Douglas J, et al. (2003). NSD1 mutations are the major cause of Sotos syndrome and occur in some cases of Weaver syndrome but are rare in other overgrowth phenotypes. *Am J Hum Genet* 72(1): 132–143.

Douglas J, et al. (2005a). Evaluation of NSD2 and NSD3 in overgrowth syndromes. *Eur J Hum Genet* 13(2): 150–153.

Douglas J, et al. (2005b). Partial NSD1 deletions cause 5% of Sotos syndrome and are readily identifiable by multiplex ligation dependent probe amplification. *J Med Genet* 42(9): e56.

Hoglund P, et al. (2003). Familial Sotos syndrome is caused by a novel 1 bp deletion of the NSD1 gene. *J Med Genet* 40(1): 51–54.

Huang N, et al. (1998). Two distinct nuclear receptor interaction domains in NSD1, a novel SET protein that exhibits characteristics of both corepressors and coactivators. *EMBO J* 17(12): 3398–3412.

Imaizumi K, et al. (2002). Sotos syndrome associated with a de novo balanced reciprocal translocation t(5;8)(q35;q24.1). *Am J Med Genet* 107(1): 58–60

Jaju RJ, et al. (2001). A novel gene, NSD1, is fused to NUP98 in the t(5;11)(q35;p15.5) in de novo childhood acute myeloid leukemia. *Blood* 98(4): 1264–1267.

Kanemoto N, et al. (2006). Nevo syndrome with an NSD1 deletion: a variant of Sotos syndrome? *Am J Med Genet A* 140(1): 70–73.

Kouzarides T (2002). Histone methylation in transcriptional control. *Curr Opin Genet Dev* 12(2): 198–209.

Kurotaki N, et al. (2001). Molecular characterization of NSD1, a human homologue of the mouse Nsd1 gene. *Gene* 279(2): 197–204.

Kurotaki N, et al. (2002). Haploinsufficiency of NSD1 causes Sotos syndrome. *Nat Genet* 30(4): 365–366.

Kurotaki N, et al. (2003). Fifty microdeletions among 112 cases of Sotos syndrome: low copy repeats possibly mediate the common deletion. *Hum Mutat* 22(5): 378–387.

Kurotaki N, et al. (2005a). Sotos syndrome common deletion is mediated by directly oriented subunits within inverted Sos-REP low-copy repeats. *Hum Mol Genet* 14(4): 535–542.

Kurotaki N, et al. (2005b). Phenotypic consequences of genetic variation at hemizygous alleles: Sotos syndrome is a contiguous gene syndrome incorporating coagulation factor twelve (FXII) deficiency. *Genet Med* 7(7): 479–483.

Melchior L, et al. (2005). dHPLC screening of the NSD1 gene identifies nine novel mutations—summary of the first 100 Sotos syndrome mutations. *Ann Hum Genet* 69(Pt 2): 222–226.

Miyake N, et al. (2003). Preferential paternal origin of microdeletions caused by prezygotic chromosome or chromatid rearrangements in Sotos syndrome. *Am J Hum Genet* 72(5): 1331–1337.

Nagai T, et al. (2003). Sotos syndrome and haploinsufficiency of NSD1: clinical features of intragenic mutations and submicroscopic deletions. *J Med Genet* 40(4): 285–289.

Nielsen AL, et al. (2004). Nizp1, a novel multitype zinc finger protein that interacts with the NSD1 histone lysine methyltransferase through a unique C2HR motif. *Mol Cell Biol* 24(12): 5184–5196.

Opitz JM, et al. (1998). The syndromes of Sotos and Weaver: reports and review. *Am J Med Genet* 79(4): 294–304.

Proud VK, et al. (1998). Weaver syndrome: autosomal dominant inheritance of the disorder. *Am J Med Genet* 79(4): 305–310.

Rahman N (2005). Mechanisms predisposing to childhood overgrowth and cancer. *Curr Opin Genet Dev* 15(3): 227–233.

Rayasam GV, et al. (2003). NSD1 is essential for early post-implantation development and has a catalytically active SET domain. *EMBO J* 22(12): 3153–3163.

Rio M, et al. (2003). Spectrum of NSD1 mutations in Sotos and Weaver syndromes. *J Med Genet* 40(6): 436–440.

Rosati R, et al. (2002). NUP98 is fused to the NSD3 gene in acute myeloid leukemia associated with t(8;11)(p11.2;p15). *Blood* 99(10): 3857–3860.

Sarimski K (2003). Behavioural and emotional characteristics in children with Sotos syndrome and learning disabilities. *Dev Med Child Neurol* 45(3): 172–178.

Schaefer GB, et al. (1997). The neuroimaging findings in Sotos syndrome. *Am J Med Genet* 68(4): 462–465.

Sotos JF, et al. (1964). Cerebral gigantism in childhood. A syndrome of excessively rapid growth and acromegalic features and a nonprogressive neurologic disorder. *N Engl J Med* 271: 109–116.

Stec I, et al. (1998). WHSC1, a 90 kb SET domain-containing gene, expressed in early development and homologous to a *Drosophila* dysmorphy gene maps in the Wolf-Hirschhorn syndrome critical region and is fused to IgH in t(4;14) multiple myeloma. *Hum Mol Genet* 7: 1071–1082.

Stec I, et al. (2000). The PWWP domain: a potential protein-protein interaction domain in nuclear proteins influencing differentiation? *FEBS Lett* 473(1): 1–5.

Tatton-Brown K, Rahman N (2004). Clinical features of NSD1-positive Sotos syndrome. *Clin Dysmorphol* 13(4): 199–204.

Tatton-Brown K, et al. (2005a). Multiple mechanisms are implicated in the generation of 5q35 microdeletions in Sotos syndrome. *J Med Genet* 4(4): 307–313.

Tatton-Brown K, et al. (2005b). Genotype-phenotype associations in Sotos syndrome: an analysis of 266 individuals with NSD1 aberrations. *Am J Hum Genet* 77(2): 193–204.

Tei S, et al. (2006). The First Japanese Familial Sotos Syndrome with a Novel Mutation of the NSD1 Gene. *Kobe J Med Sci* 52(1): 1–8.

Tong TM, et al. (2005). Spectrum of NSD1 gene mutations in southern Chinese patients with Sotos syndrome. *Chin Med J (Engl)* 118(18): 1499–1506.

Turkmen S, et al. (2003). Mutations in NSD1 are responsible for Sotos syndrome, but are not a frequent finding in other overgrowth phenotypes. *Eur J Hum Genet* 11(11): 858–865.

van Haelst MM, et al. (2005). Familial gigantism caused by an NSD1 mutation. *Am J Med Genet A* 139(1): 40–44.

Visser R, et al. (2005a). Non-hotspot-related breakpoints of common deletions in Sotos syndrome are located within destabilised DNA regions. *J Med Genet* 42(11): e66.

Visser R, et al. (2005b). Identification of a 3.0-kb major recombination hotspot in patients with Sotos syndrome who carry a common 1.9-Mb microdeletion. *Am J Hum Genet* 76(1): 52–67.

Visser R, et al. (2006). Analysis of the NSD1 promoter region in patients with a Sotos syndrome phenotype. *J Hum Genet* 51(1): 15–20.

Waggoner DJ, et al. (2005). NSD1 analysis for Sotos syndrome: insights and perspectives from the clinical laboratory. *Genet Med* 7(8): 524–533.

Weaver DD, et al. (1974). A new overgrowth syndrome with accelerated skeletal maturation, unusual facies, and camptodactyly. *J Pediatr* 84(4): 547–552.

American Journal of Medical Genetics 140A:70–73 (2006)

Nevo Syndrome With an *NSD1* Deletion: A Variant of Sotos Syndrome?

Nobuko Kanemoto,[1] Katsuyoshi Kanemoto,[1]* Gen Nishimura,[2] Tomohiro Kamoda,[3] Remco Visser,[4,5,6,7] Osamu Shimokawa,[4,7,9] and Naomichi Matsumoto[7,8]

[1]Department of Pediatrics, Ibaraki Seinan Medical Center Hospital, Sashima, Ibaraki, Japan
[2]Department of Radiology, Tokyo Metropolitan Kiyose Children's Hospital, Tokyo, Japan
[3]Department of Pediatrics, Institute of Clinical Medicine, University of Tsukuba, Tsukuba, Ibaraki, Japan
[4]Department of Human Genetics, Nagasaki University Graduate School of Biomedical Sciences, Nagasaki, Japan
[5]Department of Pediatrics, Leiden University Medical Center, Leiden, The Netherlands
[6]International Consortium for Medical Care of Hibakusha and Radiation Life Science, The 21st Century COE (Center of Excellence) Program, Nagasaki, Japan
[7]CREST, Japan Science and Technology Agency, Kawaguchi, Japan
[8]Department of Human Genetics, Yokohama City University Graduate School of Medicine, Yokohama, Japan
[9]Kyushu Medical Science Nagasaki Laboratory, Nagasaki, Japan

Received 24 September 2004; Accepted 5 March 2005

A 17-month-old girl with clinical manifestations of Nevo syndrome and *NSD1* (nuclear receptor binding SET domain protein 1) deletion is described. Nevo syndrome is a rare overgrowth syndrome showing considerable phenotypic overlap with Sotos syndrome—another, more frequent overgrowth syndrome caused by *NSD1* mutations or deletions. About a half of Japanese Sotos syndrome patients carry a 2.2-Mb common deletion encompassing *NSD1* and present with frequent brain, cardiovascular, or urinary tract anomalies. The girl we described had the common deletion and showed patent ductus arteriosus, atrial septal defect, vesicoureteral reflux, and bilateral hydronephrosis. It was thus concluded that the clinical manifestations, including the Nevo syndrome phenotype, were caused by the microdeletion. © 2005 Wiley-Liss, Inc.

Key words: Nevo syndrome; Sotos syndrome; overgrowth; *NSD1*; microdeletion

INTRODUCTION

Nevo syndrome is a rare overgrowth syndrome characterized by joint laxity, kyphosis, wrist drop, spindle shaped fingers, and volar edema, and shares many phenotypic features with Sotos syndrome [Nevo et al., 1974]. Sotos syndrome is characterized by overgrowth with advanced bone age, a dysmorphic face with macrocephaly, large hands and feet, and mental retardation [Cole and Hughes, 1994]. Recently, a 2.2-Mb microdeletion encompassing the *NSD1* gene was reported in a series of Japanese patients with Sotos syndrome [Kurotaki et al., 2003]. Patients with an *NSD1* deletion tend to have anomalies in the central nervous system (e.g., agenesis or hypoplasia of the corpus callosum), cardiovascular system (e.g., patent ductus arteriosus and atrial septal defect (ASD)), and urinary system (e.g., vesicoureteral reflux, hydronephrosis, and small kidney) [Nagai et al., 2003]. We described a young girl with Nevo syndrome with an *NSD1* deletion, and presenting with both cardiac and urinary abnormalities in addition to volar edema, and contractures of hands and feet, which are typical and pivotal features of Nevo syndrome. We postulated that the clinical manifestations in the girl, including the Nevo syndrome phenotype, were due to the microdeletion.

CLINICAL REPORT

The girl was born at full-term after an uneventful pregnancy as the first child of non-consanguineous parents. The 22-year-old father measured 170 cm and weighed 70 kg, the 19-year-old mother was 160 cm and 79 kg. Birth weight of the girl was 3,450 g (+0.4 SD), length 52 cm (+1.6 SD), and OFC 35 cm (+1.5 SD). She showed flexion contractures of hands and feet, valgus deformity of the right foot, and

*Correspondence to: Katsuyoshi Kanemoto, MD, PhD, Department of Pediatrics, Ibaraki Seinan Medical Center Hospital, Sakai 2190, Sashima, Ibaraki 306-0433, Japan. E-mail: syouni-kanemoto@seinan-mch.or.jp

DOI 10.1002/ajmg.a.30776

muscular hypotonia. Hyperbilirubinemia was treated with phototherapy for a few days. Growth, especially weight gain, was extremely accelerated. She sat alone at age 10 months and stood supported at 15 months. At age 17 months, her height was 87 cm (+3 SD), weight 13.8 kg (+3.6 SD), and OFC 48.5 cm (+1.8 SD). Motor and speech development were delayed. Although cognitive function was normal at age 17 months, she could not speak a word. When examined by us at age 17 months, generalized hypotonia and thoracic kyphosis were present. Her craniofacial features included dolichocephaly, a narrow high-arched palate, large abnormal low-set ears, and a webbed neck (Fig. 1a,b). The hands and feet were large and edematous. In addition, there was wrist drop and spindle shaped fingers (Fig. 1c,d). Echocardiography demonstrated an ASD and patent ductus arteriosus (PDA). Computed tomography of the brain showed no structural deformity. Bilateral hydronephrosis was seen on ultrasonography, and voiding cystoureterography revealed bilateral vesicoureteral reflux. Chromosome analysis revealed a normal 46,XX karyotype. At age 15 months, her bone age was advanced being 30 months, particularly seen in the metacarpophalangeal bones. Radiographic abnormalities included 11 pairs of thin ribs with a left cervical rib, thoracholumbar scoliosis, mild iliac hypoplasia, mild undermodeling of the proximal femora, and large epiphyses of the hip and knee bones.

We performed chromosomal and interphase FISH analysis on cultured peripheral blood lymphocytes from the patient using seven BAC/PAC clones encompassing *NSD1*, which detect deletions or mutations leading to Sotos syndrome [Kurotaki et al., 2003]. Five (RP11-349N15, RP11-1006E8, RP11-606E24, RP1-118M12, and RP11-147K7) of the seven clones showed a deletion in one of homologous chromosomes 5, whereas the remaining two clones (RP11-355H1 and RP11-158F10) never showed deletion (Fig. 2). Her deletion thus involved a 2.2-Mb region encompassing *NSD1* with its proximal breakpoint between RP11-355H1 and RP11-349N15, and its distal breakpoint between RP11-147K7 and RP11-158F10.

DISCUSSION

The girl we have described had clinical manifestations common to both Nevo and Sotos syndromes,

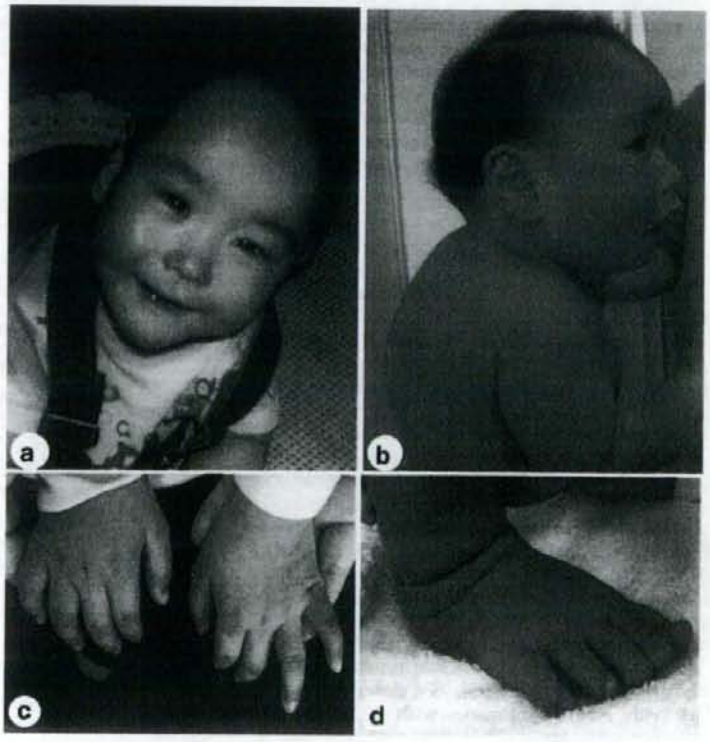

FIG. 1. The patient, (a) at age 9 months. b, c, and d: at age 17 months.

FIG. 2. FISH analysis of metaphase chromosomes from the patient. RP11-158F10 and RP11-355H1 are present (arrows), whereas RP11-349N15 and RP11-147K7 are deleted (arrowheads).

TABLE I. Phenotypic Comparison of Present and Other Patients With Nevo Syndrome or Sotos Syndrome With *NSD1* Deletions

		Patients with	
Clinical manifestations	Present patients	Nevo syndrome[a]	Sotos syndrome with deletions[b]
Common to both syndromes			
Neonatal hyperbilirubinemia	+	4/7	11/21
Retarded motor and speech development	+	2/7	9/9
Overgrowth	+	7/7	18/21
Advanced bone age	+	5/7	10/14
Coarse facial appearance	+	7/7	20/20
Prominent forehead	+	7/7	20/20
Large, low-set ears	+	6/7	16/20
High palate	+	6/7	17/18
Large hands and feet	+	5/6	20/21
Frequently seen in Sotos syndrome with deletion			
Brain anomalies	−		12/19
Cardiovascular anomalies	+[c]		12/21
Urinary tract anomalies	+[c]		7/13
Frequently seen in Nevo syndrome			
Generalized hypotonia	+	7/7	7/21
Normal head circumference	+	3/4	2/20[d]
Kyphosis	+	7/7	
Scoliosis	+	3/7	5/21
Cryptorchism		6/6	
Edema of hands and feet	+	6/7	
Wrist drop	+	7/7	
Spindle shaped fingers	+	6/6	
Valgus deformity of the feet	+	3/3	

[a]Data from Nevo et al. [1974], Hilderink and Brunner [1995], al-Gazali et al. [1997], and Dumic et al. [1998].
[b]Data from Nagai et al. [2003].
[c]PDA, ASD, vesicoureteral reflex, and hydronephrosis.
[d]Macrocephaly in 18/20 cases.

i.e., those frequently seen in Sotos syndrome patients with deletions encompassing *NSD1*, and those frequent or unique in Nevo syndrome patients (Table I). Nevo syndrome is a childhood overgrowth syndrome that shares many phenotypic features with Sotos syndrome. Identification of a common *NSD1* deletion in our patient strongly suggests that the two syndromes are either allelic. Alternatively, they may causally be related each other. In the latter case, Nevo syndrome is assumed to be an autosomal recessive disorder, and a mutant allele of the putative gene on the non-deleted chromosome 5 may be expressed through the unmasking heterozygosity mechanism by the deletion. Of seven previously reported patients with Nevo syndrome, three were two brothers and their male cousin from an inbred Arab family [Nevo et al., 1974], and two other patients were from two unrelated Arab families from different tribes [al-Gazali et al., 1997]. A male patient with the syndrome from the Netherlands was born to consanguineous parents [Hilderink and Brunner, 1995]. These findings may indicate a concentration of the syndrome among the Arab population, and support its autosomal recessive inheritance. It remains to be seen whether Nevo syndrome patients have *NSD1* mutations.

REFERENCES

al-Gazali LI, Bakalinova D, Varady E, Scorer J, Nork M. 1997. Further delineation of Nevo syndrome. J Med Genet 34:366–370.

Cole TRP, Hughes HE. 1994. Sotos syndrome: A study of the diagnostic criteria and natural history. J Med Genet 27:571–576.

Dumic M, Vukelic D, Plavsic V, Cviko A, Sokolic L, Filipovic-Grcic B. 1998. Nevo syndrome. Am J Med Genet 76:67–70.

Hilderink BGM, Brunner HG. 1995. Nevo syndrome. Clin Dysmorphol 4:319–323.

Kurotaki N, Harada N, Shimokawa O, Miyake N, Kawame H, Uetake K, Makita Y, Kondoh T, Ogata T, Hasegawa T, Nagai T, Ozaki T, Touyama M, Shenhav R, Ohashi H, Medne L, Shiihara T, Ohtsu S, Kato Z, Okamoto N, Nishimoto J, Lev D, Miyoshi Y, Ishikiriyama S, Sonoda T, Satoru S, Fukushima Y, Kurosawa K, Cheng J, Yoshiura K, Ohta T, Kishino T, Niikawa N, Matsumoto N. 2003. Fifty microdeletions among 112 cases of Sotos syndrome: Low copy repeats possibly mediate the common deletion. Hum Mutat 279:197–204.

Nagai T, Matsumoto N, Kurotaki N, Harada N, Niikawa N, Ogata T, Imaizumi K, Kurosawa K, Kondoh T, Ohashi H, Tsukahara M, Makita Y, Sugimoto T, Sonoda T, Yokoyama T, Uetake K, Sakazume S, Fukushima Y, Naritomi K. 2003. Sotos syndrome and haploinsufficiency of NSD1: Clinical features of intragenic mutations and submicroscopic deletions. J Med Genet 40:285–289.

Nevo S, Zeitzer M, Benderly A, Levy J. 1974. Evidence for autosomal recessive inheritance in cerebral gigantism. J Med Genet 25:187–190.

American Journal of Medical Genetics 140A:88–91 (2006)

Clinical Report

A Large Interstitial Deletion of 17p13.1p11.2 Involving the Smith–Magenis Chromosome Region in a Girl With Multiple Congenital Anomalies

Toshiyuki Yamamoto,[1]* Hideaki Ueda,[2] Motoyoshi Kawataki,[3] Michiko Yamanaka,[4] Toshihide Asou,[5] Yuki Kondoh,[6] Naoki Harada,[6,8] Naomichi Matsumoto,[7,8] and Kenji Kurosawa[1]

[1]Department of Medical Genetics, Kanagawa Children's Medical Center, Yokohama, Japan
[2]Department of Cardiology, Kanagawa Children's Medical Center, Yokohama, Japan
[3]Department of Neonatology, Kanagawa Children's Medical Center, Yokohama, Japan
[4]Department of Obstetrics, Kanagawa Children's Medical Center, Yokohama, Japan
[5]Department of Cardiovascular Surgery, Kanagawa Children's Medical Center, Yokohama, Japan
[6]Kyushu Medical Science Nagasaki Laboratory, Nagasaki, Japan
[7]Department of Human Genetics, Yokohama City University Graduate School of Medicine, Yokohama, Japan
[8]CREST, JST, Kawaguchi, Japan

Received 18 August 2005; Accepted 3 October 2005

A 6-month-old girl had multiple congenital anomalies, including dysmorphic face; tetralogy of Fallot, pulmonary atresia and patent ductus arteriosus; congenital cystic adenomatoid malformation of the right upper lung, and hemilateral kidney defect. Chromosome analysis as well as fluorescence in situ hybridization (FISH) and polymorphic marker analyses in the girl and her parents revealed a de novo large interstitial deletion of 17p13.1-p11.2 of the paternally derived chromosome 17. The deletion involved the Smith–Magenis chromosome region (SMCR). Lack of involvement of the Miller–Dieker syndrome region at 17p13.3 was confirmed by both FISH analysis and radiological examinations that showed no migrational abnormality. The girl died at age 7 months. This is the first report of a patient with a large interstitial deletion of 17p. © 2005 Wiley-Liss, Inc.

Key words: 17p11.2; Smith–Magenis syndrome; large interstitial deletion; dysplastic kidney; cyanotic congenital heart disease; fluorescence in situ hybridization (FISH)

INTRODUCTION

There are two major contiguous gene syndromes associated with 17p, Miller–Dieker syndrome (MDS, OMIM #247200) and Smith–Magenis syndrome (SMS, OMIM #182290), both of which have been well studied. MDS involves a subtelomeric deletion of 17p13.3 [Mutchinick et al., 1999; Cardoso et al., 2003]. Reiner et al. [1993] cloned the *LIS1* (lissencephaly-1) gene at 17p13.3, which is deleted in MDS patients. Subsequently, many single-mutations in this gene were reported to be the cause of isolated lissencephaly [Lo Nigro et al., 1997]. SMS is an interstitial deletion syndrome of 17p11.2. The mechanism of formation for this interstitial deletion is thought to be non-allelic homologous recombination between low-copy repeats (LCR) [Shaw and Lupski, 2005]. The deleted regions of SMS are usually common among patients [Shaw et al., 2004]. Slager et al. [2003] identified mutations in the *RAI1* gene, and now haploinsufficiency of *RAI1* is believed to be responsible for the behavioral, neurologic, otolaryngologic, and craniofacial abnormalities of SMS. More variable features, such as heart and renal defects, are probably due to hemizygosity of other genes involved in the 17p11.2deletion.

Recently, we encountered a girl who had a large interstitial deletion of 17p, including the Smith–Magenis chromosome region (SMCR). To our knowledge, this is the largest deletion of 17p in the literature. Here we describe the clinical details of this patient.

Grant sponsor: Japan Society for the Promotion of Science; Grant sponsor: CREST from Japan Science and Technology Agency. (JST).

*Correspondence to: Toshiyuki Yamamoto, M.D., Ph.D., IREIIMS, Tokyo Women's Medical University, 8-1 Kawada-cho, Shinjuku-ku, Tokyo 162-8666, Japan. E-mail: tyamamoto-jes@umin.ac.jp

DOI 10.1002/ajmg.a.31055

CLINICAL REPORT

A 29-year-old, primigravida woman was referred to us at 35 weeks of pregnancy because of intra-uterine growth retardation of the fetus. The woman and her 31-year-old husband were healthy and non-consanguineous. Tetralogy of Fallot (TOF) and congenital cystic adenomatoid malformation (CCAM) of the right upper lung in a fetus were suspected by prenatal ultrasonography. Caesarean was performed at 38 weeks of gestation because of breech presentation. The baby, a girl, weighted 1,978 g (−2.9 SD), and had length of 41.8 cm (−3.8 SD) and OFC of 30.6 cm (−1.7 SD). Echocardiography confirmed TOF with coarctation of the left pulmonary artery, and patent ductus arteriosus (PDA). Continuous injection of prostaglandin E1 (PGE1) was started to keep the duct open. At age 72 days, the girl received modified right Blalock-Taussig shunting operation with a Gore-Tex graft (3 mm), and her left pulmonary artery was reconstructed. Branch artery from aorta descendens was detected by chest computed tomography (CT), which confirmed CCAM of the right upper lung. Abdominal echography showed agenesis of the left kidney.

Brain MRI at age 2 months showed mild dilatation of bilateral cerebral ventricles; hypoplasia of the white matter with delayed myelination, the cerebellar vermis and of the corpus callosum, but no migrational abnormality in the cerebral cortex (Fig. 1B,D). At age 6 months, she was fed through a nasogastric tube. She followed moving objects, but instability of her neck persisted. She had upslanting palpebral fissures, low-set ears, low nasal bridge, micrognathia (Fig. 1A), a cleft palate, nuchal skin folds, a single flexion crease of the left fifth finger, bilateral single palmar creases, overlapping toes, rocker-bottom feet, sacral bossing, and a sacral dimple. She died at age 7 months of cardiac failure. Autopsy was not granted.

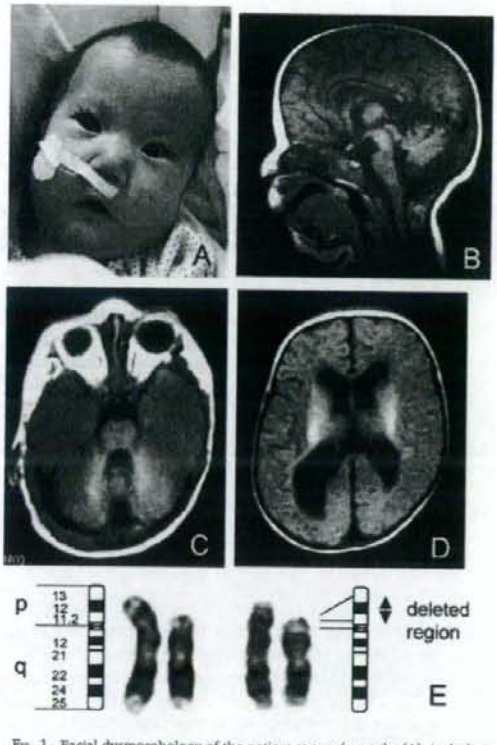

FIG. 1. Facial dysmorphology of the patient at age 4 months (**A**), including upslanting palpebral fissures, low-set ears, low nasal bridge, and micrognathia. MRI with T1W view of sagittal (**B**) and axial (**C,D**) sections at different levels, showing hypoplasia of the cerebellar vermis and corpus callosum (B), mild dilatation of bilateral cerebral ventricles with white matter hypoplasia and delayed myelination. No migrational abnormality is seen in the cerebral cortex (D). Molar tooth sign is absent (C). G-banded chromosome 17 from the patient and corresponding schematic representation (**E**). A large deletion of 17p is indicated in each right-sided chromosome.

MOLECULAR AND CYTOGENETIC STUDIES

G-banded karyotyping of cultured peripheral blood lymphocytes showed a large deletion at 17p (Fig. 1E). Fluorescence in situ hybridization (FISH) analysis by the use of LSI SMS (Vysis, Downers Grove, IL) demonstrated a deletion of the SMCR (Fig. 2A), while that with LSI LIS1 (Vysis) showed no deletion of *LIS1* (Fig. 2B). Detailed FISH analysis on interphase nuclei of the patient using BAC clone probes mapped to 17p13.3-11.2 as described elsewhere [Shimokawa et al., 2004] showed a deletion of 17p13.1-11.2 (Table I). Thus, her karyotype is interpreted as 46,XX,del(17)(p13.1p11.2).ish del(17)(LIS1+, RP1-95H6+, RP11-545O6+, RP11-457I18+, RP11-61B20+, RP11-89A15+, RP11-746E23−, RP11-125H11−, RP11-270I9−, RP11-385G5−, RP11-746E8−, RAI1−, RP1-172N16−, RP11-160E2−, RP11-363P3−, RP11-64J19−). Karyotypes of both parents were normal.

Haplotype analysis of this family was performed using the following microsatellite markers: D17S969, D17S1296, D17S2186, D17S1356, D17S1357, GATA185H04, and D17S130. Primer information was retrieved from the in-silico library [Cooperative Human Linkage Center (http://gai.nci.nih.gov/CHLC/) and UCSC Genome Bioinformatics Site (http://genome.ucsc.edu/)]. Genomic DNA was obtained from the patient and her parents, and subsequent PCR amplification was performed according to the standard method. The amplicons were visualized by ethidium bromide staining after separation by electrophoresis on an acrylamide gel. Only the result from D17S969 (located at 17p12) was informative for detecting the parental origin of the deletion. As the patient had a band for this marker in common only with her mother (Fig. 2C), it was deduced that the

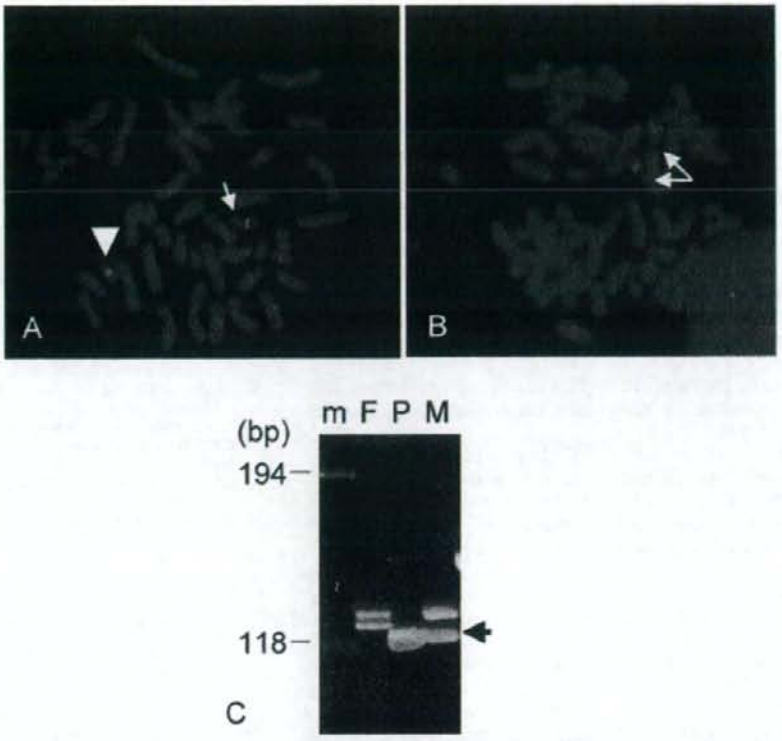

FIG. 2. Two-color FISH analysis of the patient's chromosomes using LSI SMS Spectrum Orange/RARA Spectrum Green dual-color DNA probe (**A**). Green signals were obtained by LSI RARA SpectrumGreen at band 17q21. Arrow and arrowhead indicate the presence and absence, respectively, of a signal for the SMCR. Detection of the *LIS1* region using SpectrumOrange LSI LIS1 at band 17p13.3 (**B**). Arrows indicate the presence of the *LIS1* signal. Paternal origin of the deletion (**C**). The patient inherited only the maternal allele (arrow). Electrophoretic bands of PCR products for microsatellite marker, D17S969, of the patient and her parents were visualized by ethidium bromide staining. m, marker (ϕX174/*Hae*III digest); F, father; P, patient; M, mother. [Color figure can be viewed in the online issue, which is available at www.interscience.wiley.com.]

TABLE I. BAC Clones Located to 17p13.1-11.2 Used as Probes in FISH Study

	Location				
		Nucleotide position			
Clone name	Chromosome band*	Start*	End*	Disease locus	Result of FISH
RP1-95H6	17p13.3	2443685	2535638	*LIS1*	Normal
RP11-545O6	17p13.2	3550805	3735942		Normal
RP11-457I18	17p13.2	5093178	5301854		Normal
RP11-61B20	17p13.1	6780963	6943107		Normal
RP11-89A15	17p13.1	8199810	8365717		Normal
RP11-746E23	17p13.1	8576926	8748280		Deletion
RP11-125H11	17p13.1	9176082	9364840		Deletion
RP11-270I9	17p13.1	9745074	9904704		Deletion
RP11-385G5	17p12	11132724	11344170		Deletion
RP11-746E8	17p12	12435731	12620614		Deletion
RP11-172N16	17p11.2	18069802	18201100	*SMS*	Deletion
RP11-160E2	17p11.2	18863814	19021902		Deletion
RP11-363P3	17p11.2	20012562	20185625		Deletion
RP11-64J19	17p11.2	21014522	21191548		Deletion

*Chromosomal location or nucleotide position are from UCSC database (May 2004).

paternally derived allele at this locus was deleted in the patient.

DISCUSSION

The girl described here had a de novo large interstitial deletion of 17p13.1-11.2, including the SMCR, on the paternally derived chromosome 17. The lack of clinical manifestations for MDS, including lissencephaly was confirmed by molecular cytogenetic analysis, that is, the *LIS1* region, which is critical for MDS, was intact. Hereditary neuropathy with liability to pressure palsies (HNPP) can be caused by a deletion of the *PMP22* (peripheral myelin protein-22) gene that should be included in her deletion extent. However, since the age of onset of HNPP is usually between 15 and 20 years, she was too young to present the symptoms for the disease such as neuropathy.

The patient had facial dysmorphism showing a broad, flat nasal bridge; upslanting palpebral fissures, sparse eyebrows, broad midface, and cleft palate. These manifestations are characteristic of typical of SMS [Greenberg et al., 1991]. Other facial anomalies such as a long philtrum and a carp-shaped mouth, and hemilateral dysplasia of the kidney have not been reported in SMS patients. It is likely that these abnormalities were due to hemizygosity of genes other than those in the SMCR. Severe congenital heart disease (CHG) of the patient, including TOF, PA, and VSD, is also compatible with SMS. Greenberg et al. [1996] described that at least 37% of SMS patients had CHG, and some patients were reported to have TOF, PA, and VSD [Smith et al., 1986; Wong et al., 2003; Myers and Challman, 2004]. Thus, the heart anomalies in our patient are not exceptional for SMS. Natacci et al. [2000] described a patient who had SMS associated with Joubert syndrome. Our patient also had hypoplasia of the cerebellar vermis but molar tooth sign was not identified by MRI. Thus, Joubert syndrome was ruled out in our case.

In conclusion, this is, to our knowledge, the first report of a large deletion of 17p. From our experience with this patient, such a deletion may lead to a poor prognosis, early infantile lethality. Our case may contribute to better understanding of a genotype–phenotype correlation of SMS.

ACKNOWLEDGMENTS

This work was supported through a special grant from Japan Society for the Promotion of Science.

REFERENCES

Cardoso C, Leventer RJ, Ward HL, Toyo-Oka K, Chung J, Gross A, Martin CL, Allanson J, Pilz DT, Olney AH, Mutchinick OM, Hirotsune S, Wynshaw-Boris A, Dobyns WB, Ledbetter DH. 2003. Refinement of a 400-kb critical region allows genotypic differentiation between isolated lissencephaly, Miller-Dieker syndrome, and other phenotypes secondary to deletions of 17p13.3. Am J Hum Genet 72:918–930.

Greenberg F, Guzzetta V, Montes de Oca-Luna R, Magenis RE, Smith ACM, Richter SF, Kondo I, Dobyns WB, Patel PI, Lupski JR. 1991. Molecular analysis of the Smith-Magenis syndrome: A possible contiguous-gene syndrome associated with del(17)(p11.2). Am J Hum Genet 49:1207–1218.

Greenberg F, Lewis RA, Potocki L, Glaze D, Parke J, Killian J, Murphy MA, Williamson D, Brown F, Dutton R, McCluggage C, Friedman E, Sulek M, Lupski JR. 1996. Multi-disciplinary clinical study of Smith-Magenis syndrome (deletion 17p11.2). Am J Med Genet 62:247–254.

Lo Nigro C, Chong CS, Smith AC, Dobyns WB, Carrozzo R, Ledbetter DH. 1997. Point mutations and an intragenic deletion in LIS1, the lissencephaly causative gene in isolated lissencephaly sequence and Miller-Dieker syndrome. Hum Mol Genet 6:157–164.

Mutchinick OM, Shaffer LG, Kashork CD, Cervantes EI. 1999. Miller-Dieker syndrome and trisomy 5p in a child carrying a derivative chromosome with a microdeletion in 17p13.3 telomeric to the LIS1 and the D17S379 loci. Am J Med Genet 85:99–104.

Myers SM, Challman TD. 2004. Congenital heart defects associated with Smith-Magenis syndrome: Two cases of total anomalous pulmonary venous return. Am J Med Genet 131A: 99–100.

Natacci F, Corrado L, Pierri M, Rossetti M, Zuccarini C, Riva P, Miozzo M, Larizza L. 2000. Patient with large 17p11.2 deletion presenting with Smith-Magenis syndrome and Joubert syndrome phenotype. Am J Med Genet 95:467–472.

Reiner O, Carrozzo R, Shen Y, Wehnert M, Faustinella F, Dobyns WB, Caskey CT, Ledbetter DH. 1993. Isolation of a Miller-Dieker lissencephaly gene containing G protein beta-subunit-like repeats. Nature 364:717–721.

Shaw CJ, Lupski JR. 2005. Non-recurrent 17p11.2 deletions are generated by homologous and non-homologous mechanisms. Hum Genet 116:1–7.

Shaw CJ, Withers MA, Lupski JR. 2004. Uncommon deletions of the Smith-Magenis syndrome region can be recurrent when alternate low-copy repeats act as homologous recombination substrates. Am J Hum Genet 75:75–81.

Shimokawa O, Kurosawa K, Ida T, Harada N, Kondoh T, Miyake N, Yoshiura K, Kishino T, Ohta T, Niikawa N, Matsumoto N. 2004. Molecular characterization of inv dup del(8p): Analysis of five cases. Am J Med Genet Part A 128A:133–137.

Slager RE, Newton TL, Vlangos CN, Finucane B, Elsea SH. 2003. Mutations in RAI1 associated with Smith-Magenis syndrome. Nature Genet 33:466–468.

Smith ACM, McGavran L, Robinson J, Waldstein G, Macfarlane J, Zonana J, Reiss J, Lahr M, Allen L, Magenis E. 1986. Interstitial deletion of (17)(p11.2p11.2) in nine patients. Am J Med Genet 24:393–414.

Wong JT, Chan DK, Wong KY, Tan M, Rudduck C, Tien SL. 2003. Smith-Magenis syndrome and cyanotic congenital heart disease: A case report. Clin Dysmorphol 12: 73–74.

American Journal of Medical Genetics 140A:291–293 (2006)

Research Letter

No Detectable Genomic Aberrations by BAC Array CGH in Kabuki Make-Up Syndrome Patients

Noriko Miyake,[1,2,3,19] Osamu Shimokawa,[1,3,4] Naoki Harada,[1,3,4] Nadia Sosonkina,[1,3] Aiko Okubo,[1] Hiroki Kawara,[4] Nobuhiko Okamoto,[5] Hirofumi Ohashi,[6] Kenji Kurosawa,[7] Kenji Naritomi,[8] Tadashi Kaname,[8] Toshiro Nagai,[9] Vorasuk Shotelersuk,[10] Jia-Woei Hou,[11] Yoshimitsu Fukushima,[12] Tatsuro Kondoh,[2] Tadashi Matsumoto,[13] Toshihiko Shinoki,[14] Mitsuhiro Kato,[15] Hidefumi Tonoki,[16] Masayo Nomura,[1,3] Ko-ichiro Yoshiura,[1,3] Tatsuya Kishino,[3,17] Tohru Ohta,[3,18] Norio Niikawa,[1,3] and Naomichi Matsumoto [3,19]*

[1]Department of Human Genetics, Nagasaki University Graduate School of Biomedical Sciences, Nagasaki, Japan
[2]Department of Pediatrics, Nagasaki University Graduate School of Biomedical Sciences, Nagasaki, Japan
[3]CREST, Japan Science and Technology Agency, Kawaguchi, Japan
[4]Kyushu Medical Science Nagasaki Laboratory, Nagasaki, Japan
[5]Department of Planning and Research, Osaka Medical Center and Research Institute for Maternal and Child Health, Izumi, Japan
[6]Division of Medical Genetics, Saitama Children's Medical Center, Iwatsuki, Japan
[7]Division of Medical Genetics, Kanagawa Children's Medical Center, Yokohama, Japan
[8]Department of Medical Genetics, University of the Ryukyus School of Medicine, Nishihara, Japan
[9]Department of Pediatrics, Koshigaya Hospital, Dokkyo University School of Medicine, Koshigaya, Japan
[10]Department of Pediatrics, Faculty of Medicine, Chulalongkorn University and Hospital, Bangkok, Thailand
[11]Department of Pediatrics, Division of Medical Genetics/Metabolism, Chang Gung Children's Hospital, Taoyuan, Taiwan
[12]Department of Medical Genetics, Shinshu University School of Medicine, Matsumoto, Japan
[13]Department of Nursing, Nagasaki University School of Health Sciences, Nagasaki, Japan
[14]Department of Pediatrics, Mie University School of Medicine, Tsu, Japan
[15]Department of Pediatrics, Yamagata University School of Medicine, Yamagata, Japan
[16]Department of Pediatrics, Hokkaido University School of Medicine, Sapporo, Japan
[17]Division of Functional Genomics, Center for Frontier Life Sciences, Nagasaki University, Nagasaki, Japan
[18]The Research Institute of Personalized Health Sciences, Health Sciences University of Hokkaido, Ishikari-tobetsu, Japan
[19]Department of Human Genetics, Yokohama City University Graduate School of Medicine, Yokohama, Japan

Received 24 May 2005; Accepted 28 August 2005

To the Editor:

Kabuki make-up syndrome (KMS, OMIM 147920), independently established by Niikawa et al. [1981] and Kuroki et al. [1981], is characterized by characteristic facial features resembling the Kabuki actor's make-up, mild to moderate mental retardation, postnatal growth retardation, skeletal abnormalities, and unusual dermatoglyphic patterns [Matsumoto and Niikawa, 2003]. The multisystem involvement of the KMS phenotype suggests that KMS is caused by a microdeletion or microduplication involving several genes. Milunsky and Huang [2003] reported that all of the six KMS patients they examined had approximate 3.5-Mb duplication at 8p22–p23.1 revealed by comparative genomic hybridization (CGH) and fluorescence in situ hybridization (FISH). They also suggested that a paracentric inversion in mothers, detected by RP11-122N11, might contribute to the occurrence of the syndrome. At least three groups, including us, failed to replicate their results by FISH and/or array CGH analysis [Miyake et al., 2004; Engelen et al., 2005; Hoffman et al., 2005]. Schoumans et al. [2005] reported that they observed no chromosomal abnormalities in 10 affected Caucasian individuals with typical KMS using the 1.2-Mb-resolution whole genome BAC array.

Grant sponsor: The Ministry of Education, Culture, Sports, Science, and Technology of Japan; Grant number: 16390101; Grant sponsor: Ministry of Health, Labour and Welfare (Research Grant 15B-4); Grant sponsor: CREST from Japan Science and Technology Agency (JST).

*Correspondence to: Naomichi Matsumoto, Department of Human Genetics, Yokahama City University Graduate School of Medicine, Fukuura 3-9, Kanazawa-ku, Yokohama 236-0004, Japan.
E-mail: naomat@yokohama-cu.ac.jp

DOI 10.1002/ajmg.a.31012

Using a newly developed BAC array covering the whole genome with a 1.5-Mb resolution, in this study, array CGH (aCGH) was performed in 38 patients with typical KMS to find genomic imbalances in relation to KMS. Detailed experimental protocols are described elsewhere [Miyake et al., 2005]. Peripheral blood leukocytes or lymphoblastoid cell lines from the 38 patients (20 males and 18 females) and their parents when available were sent to us after informed consent. All KMS cases were sporadic and had a normal karyotype according to G-banded chromosomal analysis at the 400-band level. Their metaphase chromosomes for FISH and DNA for aCGH were prepared either from immortalized lymphoblastoid cell lines or peripheral blood leukocytes according to standard protocols.

We detected a total of 115 clones implying occult genomic imbalances, which were all subsequently confirmed by FISH (14 clones as deletions and 101 clones as duplications) (Fig. 1). Heterozygous deletion/duplication might be associated with the pathogenesis of KMS, because an autosomal (or pseudoautosomal) dominant inheritance is suspected in KMS [Matsumoto and Niikawa, 2003]. All copy number changed loci (clones) observed in this series of KMS patients, except four loci, were unlikely to be associated with KMS, because the same changes were also observed in either of their healthy parents, and/or non-KMS individuals with non-syndromic mental retardation [Miyake et al., 2005], and/or were registered in the Database of Genomic Variants (http://projects.tcag.ca/variation/). One heterozygous deletion at RP11-97F19 (2p11.2) in two patients (KMS5 and KMS17), and two heterozygous duplications at RP11-418N20 (Xp22.33) and RP4-617A9 (Xp22.3) in a patient (KMS14) remain inconclusive, because parental samples were unavailable. These changes in the three patients are described in detail below. Among 37 loci showing copy number changes in KMS patients, a total of 11 loci were already registered as copy number polymorphisms (CPNs) in the Database of Genomic Variants (checked on July 19, 2005) (Fig. 1), confirming that these changes are unlikely pathogenic.

RP11-97F19 Deletion at 2p11.2 in KMS5 and KMS17

We delimited the deletion to an approximate 1-Mb region from RP11-15J7 to RP11-136K15 by detailed

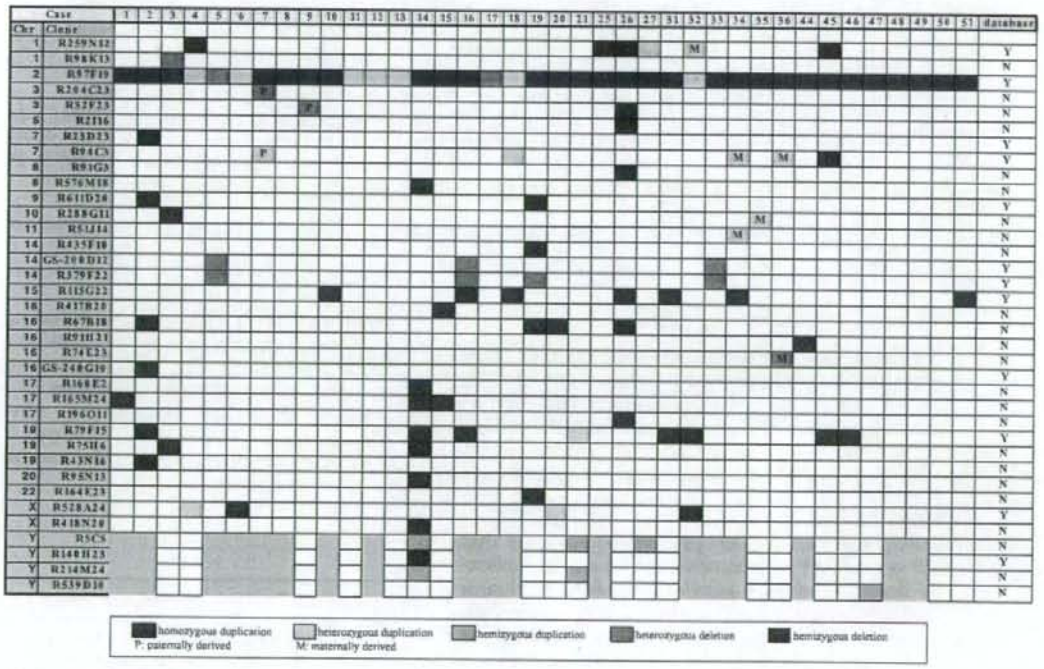

FIG. 1. Summary of BAC array CGH and FISH studies on KMS patients. Top yellow row indicates KMS patients (male in black, and female in red). Left green columns show information of clone IDs and their chromosomal locations. Duplications are shown as in red (homozygous) and orange (heterozygous). Deletions are in pale-blue (heterozygous) and dark-blue (hemizygous). Parental origin of changes is indicated as P (paternal) and M (maternal). No de novo changes were confirmed. Y in right column indicates clone/locus registered as copy number variation (CPN) locus in the Database of Genomic Variants (http://projects.tcag.ca/variation/). N clone/locus not registered in the database.

FISH analysis [UCSC Genome Browser NCBI build 35 (May 2004) coordinates, chromosome 2 nucleotide 88979594–89962288 bp] (data not shown). The gain of this region was reported previously [Sebat et al., 2004] and is described at the Database of Genomic Variants (http://projects.tcag.ca/variation), but the loss has never been reported. We did not find any cases with the same deletion in 200 chromosomes of normal Japanese controls. Regarding the duplication, homozygous and heterozygous duplication were found in 92 and 8 controls, respectively. The allele frequencies of the duplication in KMS and normal controls were 87.5% and 96%, respectively. No established genes exist within the deletion.

RP4-617A9 and RP11-418N20 Duplication at Xp22.3 in KMS14

RP4-617A9 and RP11-418N20 are closely located ~0.12 Mb apart. The heterozygous duplication of RP4-617A9 and RP11-418N20 in KMS14 was observed by aCGH. FISH analysis revealed that the duplication spans about 0.7 Mb from RP11-794A12 (distal) to RP11-418N20 (proximal) (UCSC coordinates, chromosome X nucleotide 2341315–3106243). None of 98 chromosomes in normal Japanese controls possessed the duplication. In addition, the gain of this region has not been reported yet at Database of Genome Variants. This region was overlapped with a part of the pseudoautosomal region 1 (PAR1). Among seven genes mapped to the duplication, *ZBED1* and *CD99* were in PAR1. Though they are attractive candidate genes according to a pseudoautosomal dominant inheritance hypothesis [Matsumoto and Niikawa, 2003], we could only find three SNPs in *CD99* [68A > G (D23G), 496A > G (M166V), 518A > T (N173I)], but no pathological nucleotide changes of the two genes in 37 other KMS patients (data not shown).

In conclusion, our study of 38 KMS patients did not show any pathological copy number changes, similar to the previous report [Schoumans et al., 2005]. Thus, it is less likely that microdeletions/duplications are frequent pathological changes in KMS. KMS may be caused by defects of a single gene that regulates various target genes/organs.

ACKNOWLEDGMENTS

The authors are greatly indebted to the patients and their parents. We express our gratitude to Ms. Yasuko Noguchi, Kazumi Miyazaki, and Naoko Yanai for their excellent technical assistance. We express our special thanks to Dr. Norio Takahashi for extracting a part of BAC DNAs. The Ministry of Education, Culture, Sports, Science, and Technology of Japan (No. 16390101) and the Ministry of Health, Labour and Welfare (Research Grant 15B-4) for N. M.; CREST from Japan Science and Technology Agency (JST) for N. N.

REFERENCES

Engelen JJ, Loneus WH, Vaes-Peeters G, Schrander-Stumpel CT. 2005. Kabuki syndrome is not caused by an 8p duplication: A cytogenetic study in 20 patients. Am J Med Genet A 132A:276–277.

Hoffman JD, Zhang Y, Greshock J, Ciprero KL, Emanuel BS, Zackai EH, Weber BL, Ming JE. 2005. Array based CGH and FISH fail to confirm duplication of 8p22-p23.1 in association with Kabuki syndrome. J Med Genet 42:49–53.

Kuroki Y, Suzuki Y, Chyo H, Hata A, Matsui I. 1981. A new malformation syndrome of long palpebral fissures, large ears, depressed nasal tip, and skeletal anomalies associated with postnatal dwarfism and mental retardation. J Pediatr 99:570–573.

Matsumoto N, Niikawa N. 2003. Kabuki make-up syndrome: A review. Am J Med Genet C Semin Med Genet 117C:57–65.

Milunsky JM, Huang XL. 2003. Unmasking Kabuki syndrome: Chromosome 8p22-8p23.1 duplication revealed by comparative genomic hybridization and BAC-FISH. Clin Genet 64:509–516.

Miyake N, Harada N, Shimokawa O, Ohashi H, Kurosawa K, Matsumoto T, Fukushima Y, Nagai T, Shotelersuk V, Yoshiura K, Ohta T, Kishino T, Niikawa N, Matsumoto N. 2004. On the reported 8p22-p23.1 duplication in Kabuki make-up syndrome (KMS) and its absence in patients with typical KMS. Am J Med Genet A 128A:170–172.

Miyake N, Shimokawa O, Harada N, Sosonkina N, Okubo A, Kawara H, Okamoto N, Kurosawa K, Kawame H, Iwakoshi M, Kosho T, Fukushima Y, Makita Y, Yokoyama Y, Yamagata T, Kato M, Hiraki Y, Nomura M, Yoshiura K-I, Kishino T, Ohta T, Mizuguchi T, Niikawa N, Matsumoto N. 2005. BAC array CGH reveals genomic aberrations in non-syndromic mental retardation. Am J Med Genet (this issue).

Niikawa N, Matsuura N, Fukushima Y, Ohsawa T, Kajii T. 1981. Kabuki make-up syndrome: A syndrome of mental retardation, unusual facies, large and protruding ears, and postnatal growth deficiency. J Pediatr 99:565–569.

Schoumans J, Nordgren A, Ruivenkamp C, Brondum-Nielsen K, Teh BT, Anneren G, Holmberg E, Nordenskjold M, Anderlid BM. 2005. Genome-wide screening using array-CGH does not reveal microdeletions/microduplications in children with Kabuki syndrome. Eur J Hum Genet 13:260–263.

Sebat J, Lakshmi B, Troge J, Alexander J, Young J, Lundin P, Maner S, Massa H, Walker M, Chi M, Navin N, Lucito R, Healy J, Hicks J, Ye K, Reiner A, Gilliam TC, Trask B, Patterson N, Zetterberg A, Wigler M. 2004. Large-scale copy number polymorphism in the human genome. Science 305:525–528.

American Journal of Medical Genetics 140A:205–211 (2006)

BAC Array CGH Reveals Genomic Aberrations in Idiopathic Mental Retardation

Noriko Miyake,[1,2,3,17] Osamu Shimokawa,[1,3,4] Naoki Harada,[1,3,4] Nadia Sosonkina,[1,3] Aiko Okubo,[1] Hiroki Kawara,[4] Nobuhiko Okamoto,[5] Kenji Kurosawa,[6] Hiroshi Kawame,[7] Mie Iwakoshi,[8] Tomoki Kosho,[9] Yoshimitsu Fukushima,[9] Yoshio Makita,[10] Yuji Yokoyama,[11] Takanori Yamagata,[12] Mitsuhiro Kato,[13] Yoko Hiraki,[14] Masayo Nomura,[1,3] Ko-ichiro Yoshiura,[1,3] Tatsuya Kishino,[3,15] Tohru Ohta,[3,16] Takeshi Mizuguchi,[3,17] Norio Niikawa,[1,3] and Naomichi Matsumoto[3,17]*

[1]Department of Human Genetics, Nagasaki University Graduate School of Biomedical Sciences, Nagasaki, Japan
[2]Department of Pediatrics, Nagasaki University Graduate School of Biomedical Sciences, Nagasaki, Japan
[3]CREST, Japan Science and Technology Agency, Kawaguchi, Japan
[4]Kyushu Medical Science Nagasaki Laboratory, Nagasaki, Japan
[5]Department of Planning and Research, Osaka Medical Center and Research Institute for Maternal and Child Health, Izumi, Japan
[6]Division of Medical Genetics, Kanagawa Children's Medical Center, Yokohama, Japan
[7]Division of Medical Genetics, Nagano Children Hospital, Minamiazumi-gun, Japan
[8]Nishinomiya Municipal Wakaba-en, Nishinomiya, Japan
[9]Department of Medical Genetics, Shinshu University School of Medicine, Matsumoto, Japan
[10]Department of Pediatrics, Asahikawa Medical Collage, Asahikawa, Japan
[11]Department of Pediatrics, Faculty of Medicine, Okayama University Medical School, Okayama, Japan
[12]Department of Pedicatrics, Jichi Medical School, Kawachi-gun, Japan
[13]Department of Pedicatrics, Yomagata University School of Medicine, Yamagata, Japan
[14]Hiroshima Municipal Center for Child Health and Development, Hiroshima, Japan
[15]Division of Functional Genomics, Center for Frontier Life Sciences, Nagasaki University, Nagasaki, Japan
[16]The Research Institute of Personalized Health Sciences, Health Sciences University of Hokkaido, Ishikari-tobetsu, Japan
[17]Department of Human Genetics, Yokohama City University Graduate School of Medicine, Yokohama, Japan

Received 18 August 2005; Accepted 29 November 2005

Array using 2,173 BAC clones covering the whole human genome has been constructed. All clones spotted were confirmed to show a unique signal at the predicted chromosomal location by FISH analysis in our laboratory. A total of 30 individuals with idiopathic mental retardation (MR) were analyzed by comparative genomic hybridization using this array. Three deletions, one duplication, and one unbalanced translocation could be detected in five patients, which are likely to contribute to MR. The constructed array was shown to be an efficient tool for the detection of pathogenic genomic rearrangements in MR patients as well as copy number polymorphisms (CPNs).

Key words: mental retardation; BAC array CGH; FISH; chromosomal abnormality

INTRODUCTION

Mental retardation (MR) occurs with the prevalence of 2%~3% of general population [Knight et al., 1999]. Chromosomal rearrangements at subtelomeric regions have been detected in 5%~6% of affected individuals with MR [Flint et al., 1995; Knight et al., 1999; de Vries et al., 2001, 2003; Harada et al., 2004], and the whole genome array comparative genomic hybridization (aCGH) with an approximate 1-Mb resolution detected pathological genomic imbalances in 14%–20% of MR cases [Vissers et al., 2003; Shaw-Smith et al., 2004], implying that aCGH is an

Grant sponsor: The Ministry of Education, Culture, Sports, Science, and Technology of Japan; Grant number: 16390101; Grant sponsor: The Ministry of Health, Labour and Welfare; Grant number: 15B-4; Grant sponsor: CREST from Japan Science and Technology Agency (JST).

*Correspondence to: Dr. Naomichi Matsumoto, Department of Human Genetics, Yokohama City University Graduate School of Medicine, Fukuura 3-9, Kanazawa-ku, Yokohama 236-0004, Japan.
E-mail: naomat@yokohama-cu.ac.jp

DOI 10.1002/ajmg.a.31098

essential method to detect submicroscopic chromosomal abnormalities in patients with idiopathic learning disabilities.

We have developed a new BAC array system covering the whole genome with a 1.4-Mb resolution after eliminating problematic clones with multiple and/or erroneous FISH signals in our laboratory. Thus all clones used for this array were confirmed to show a unique signal at a predicted chromosomal position. Using this system, aCGH was performed in 30 idiopathic MR to validate genomic imbalances in relation to MR. Several chromosomal abnormalities as well as copy number polymorphisms (CPNs) we could find will be presented.

MATERIALS AND METHODS

Subjects

Peripheral blood leukocytes or lymphoblastoid cell lines from 30 cases of idiopathic MR associated with some dysmorphic features (14 males and 16 females) and their parents, when available, were sent to us after informed consent. MR patients, except for sisters, MR123 and MR124, were sporadic. One phenotypic female MR case, MR118 with showed obvious cytogenetic abnormality, 46,XY, but other MR cases had a normal karyotype according to G-banded chromosomal analysis at the 400-band level. Their metaphase chromosomes for FISH and DNA for aCGH were prepared according to standard protocols. We also used DNA from an individual with an abnormal karyotype [46,XX,inv dup del(8)(qter → p23.1::p23.1 → p11.23:)] for a positive control, and from a normal male and a female as sex-matched references.

Degenerate Oligonucleotide Primed PCR (DOP-PCR)

BAC/PAC DNA was amplified by two-step PCR. First DOP-PCR was performed using three different primers [Fiegler et al., 2003] as previously described [Harada et al., 2004]. The second 5′-amino-linked primer (5′-GGAAACAGCccgactcgag-3′) whose 3′ 10 base-pairs (small character) are the same as 5′ 10 base-pairs of the first DOP-PCR primers. The second PCR was performed in a total volume of 100 μl containing 1 μl of the mixture of the three different first-PCR products, 1 × Ex Taq buffer, 5 U Ex Taq (Takara, Ohtsu, Japan), 0.2 mmol/L each dNTP, and 1 μmol/L second DOP-PCR primer, and the PCR was cycled 35 times at 94°C for 30 sec, 50°C for 30 sec, and 72°C for 8 min. These four primers were purchased from Hokkaido System Science Co. Ltd. (Sapporo, Japan).

Whole Genome Array

We selected 2,505 "FISHed" BAC/PAC clones using UCSC genome browser [2003 July version (http://genome.ucsc.edu/cgi-bin/hgGateway)], spacing at every 1.4 Mb of the whole human genome and chose 2,173 clones as they showed a unique signal at the predicted chromosomal location. A total of 332 clones were not used for array study, as 172 yielded multiple chromosomal signals by FISH (6.8%) and 160 showed an aberrant signal that is probably due to contamination (6.4%). Fifty-nine BAC/PAC clones previously used for subtelomere and syndromic MR-specific microarray [Harada et al., 2004; Kurosawa et al., 2004] were also incorporated into 2,173 clones. BAC/PAC DNA was extracted using an automatic DNA extraction system PI-100 (Kurabo, Osaka, Japan), amplified by two-round PCR, purified and adjusted to the final concentration >500 ng/μl, and spotted in duplicate on CodeLink™ activated slides (Amersham Biosciences Corp, Piscataway, NJ) by the ink-jet spotting method (Nihon Gaishi, Nagoya, Japan). The identical set of duplicated spots was printed twice as block A and block B on one slide.

FISH

BAC/PAC DNA was labeled with SpectrumGreen™-11-dUTP or SpectrumOrange™-11-dUTP (Vysis, Downers Grove, IL) by nick translation, and denatured at 70°C for 10 min. Probe-hybridization mixtures (15 μl) were applied on chromosomes, incubated at 37°C for 16–72 hr, then washed and mounted in antifade solution (Vector, Burlingame, CA) containing DAPI. Fluorescence photomicroscopy was performed as previously described [Miyake et al., 2004].

Array CGH

After complete digestion using *Eco*RI, subject's DNA was labeled with Cy-3 dCTP (Amersham Biosciences) and reference DNA was labeled with Cy-5 dCTP (Amersham Biosciences) using DNA random primer Kit (Invitrogen, Carlsbad, CA) (CGH1). Dyes were swapped in CGH2 (subject DNA with Cy5 and reference DNA with Cy3) to check whether signal patterns of CGH1 were reversed for ruling out false positives. Prehybridization and hybridization were preformed as previously described [Harada et al., 2004]. Slides were incubated at 37°C for 72 hr with gentle shaking and were washed once with solution A (1 × PBS with 0.05% Tween 20), and twice with solution B (2 × SSC with 50% Formamide) at 43°C for 15 min, and twice with solution A at room temperature for 10 min with gently shaking. After drying, the arrays were scanned by GenePix 4000B (Axon Instruments, Union City, CA) and analyzed using GenePix Pro 4.0 (Axon Instruments).

The signal intensity ratio between patient's and control DNA was calculated from the data of the